

Loss-of-Function Mutations of *ILDR1* Cause Autosomal-Recessive Hearing Impairment *DFNB42*

Guntram Borck,^{1,2,*} Atteeq Ur Rehman,^{3,4,29} Kwanghyuk Lee,^{5,29} Hans-Martin Pogoda,^{6,29} Naseebullah Kakar,^{7,29} Simon von Ameln,^{1,2,8} Nicolas Grillet,⁹ Michael S. Hildebrand,¹⁰ Zubair M. Ahmed,¹¹ Gudrun Nürnberg,^{2,12,13} Muhammad Ansar,¹⁴ Sulman Basit,¹⁴ Qamar Javed,¹⁴ Robert J. Morell,³ Nabilah Nasreen,⁷ A. Eliot Shearer,¹⁰ Adeel Ahmad,¹⁵ Kimia Kahrizi,¹⁶ Rehan S. Shaikh,^{4,17} Rana A. Ali,⁴ Shaheen N. Khan,⁴ Ingrid Goebel,^{1,2,8} Nicole C. Meyer,¹⁰ William J. Kimberling,¹⁸ Jennifer A. Webster,¹⁹ Dietrich A. Stephan,^{20,21,22} Martin R. Schiller,²³ Melanie Bahlo,²⁴ Hossein Najmabadi,¹⁶ Peter G. Gillespie,²⁵ Peter Nürnberg,^{2,12,13} Bernd Wollnik,^{1,2,13} Saima Riazuddin,²⁶ Richard J.H. Smith,^{10,27} Wasim Ahmad,¹⁴ Ulrich Müller,⁹ Matthias Hammerschmidt,^{2,6,13} Thomas B. Friedman,³ Sheikh Riazuddin,²⁸ Suzanne M. Leal,⁵ Jamil Ahmad,⁷ and Christian Kubisch^{1,2,8,13}

By using homozygosity mapping in a consanguineous Pakistani family, we detected linkage of nonsyndromic hearing loss to a 7.6 Mb region on chromosome 3q13.31-q21.1 within the previously reported *DFNB42* locus. Subsequent candidate gene sequencing identified a homozygous nonsense mutation (c.1135G>T [p.Glu379X]) in *ILDR1* as the cause of hearing impairment. By analyzing additional consanguineous families with homozygosity at this locus, we detected *ILDR1* mutations in the affected individuals of 10 more families from Pakistan and Iran. The identified *ILDR1* variants include missense, nonsense, frameshift, and splice-site mutations as well as a start codon mutation in the family that originally defined the *DFNB42* locus. *ILDR1* encodes the evolutionarily conserved immunoglobulin-like domain containing receptor 1, a putative transmembrane receptor of unknown function. In situ hybridization detected expression of *Ildr1*, the murine ortholog, early in development in the vestibule and in hair cells and supporting cells of the cochlea. Expression in hair cell- and supporting cell-containing neurosensory organs is conserved in the zebrafish, in which the *ildr1* ortholog is prominently expressed in the developing ear and neuromasts of the lateral line. These data identify loss-of-function mutations of *ILDR1*, a gene with a conserved expression pattern pointing to a conserved function in hearing in vertebrates, as underlying nonsyndromic prelingual sensorineural hearing impairment.

Introduction

Hearing is mediated by highly specialized cell types within the inner ear that ultimately convert sound into electrical signals. The high degree of conservation of hearing processes in vertebrates is reflected by homologies in the anatomy of the ear as well as by the conservation of molecular pathways underlying hearing and balance.¹ Sound is

transduced by hair cells embedded in layers of supporting cells and the resulting electrical signal is then transmitted to specific areas of the brain for information processing. Any perturbation of the development, structure, function, or maintenance of hair cells, supporting cells, or the auditory nerve can lead to hearing impairment.^{2–4}

In humans, hearing impairment can be due to environmental influences, but in industrialized countries most

¹Institute of Human Genetics, University of Cologne, 50931 Cologne, Germany; ²Center for Molecular Medicine Cologne (CMMC), University of Cologne, 50931 Cologne, Germany; ³Laboratory of Molecular Genetics, National Institute on Deafness and Other Communication Disorders, National Institutes of Health, Rockville, MD 20850, USA; ⁴National Centre of Excellence in Molecular Biology, University of the Punjab, Lahore 54500, Pakistan; ⁵Department of Molecular and Human Genetics, Baylor College of Medicine, Houston, TX 77030, USA; ⁶Institute for Developmental Biology, University of Cologne, 50674 Cologne, Germany; ⁷Department of Biotechnology and Informatics, BUITEMS, Quetta 78300, Pakistan; ⁸Institute of Human Genetics, University of Ulm, 89081 Ulm, Germany; ⁹Dorris Neuroscience Center and Department of Cell Biology, The Scripps Research Institute, La Jolla, CA 92037, USA; ¹⁰Department of Otolaryngology, Head and Neck Surgery, University of Iowa, Iowa City, IA 52242, USA; ¹¹Division of Pediatric Ophthalmology, Cincinnati Children's Hospital Research Foundation, and the Department of Ophthalmology, College of Medicine, University of Cincinnati, OH 45229, USA; ¹²Cologne Center for Genomics (CCG), University of Cologne, 50931 Cologne, Germany; ¹³Cologne Excellence Cluster on Cellular Stress Responses in Aging-Associated Diseases (CECAD), University of Cologne, 50674 Cologne, Germany; ¹⁴Department of Biochemistry, Faculty of Biological Sciences, Quaid-I-Azam University, Islamabad 45320, Pakistan; ¹⁵King Edward Medical University, Mayo Hospital, Lahore 54000, Pakistan; ¹⁶Genetics Research Center, University of Social Welfare and Rehabilitation Sciences, Tehran 19834, Iran; ¹⁷Institute of Biotechnology, Bahauddin Zakariya University, Multan 60800, Pakistan; ¹⁸Department of Genetics, Boys Town National Research Hospital, Omaha, NE 68131, USA; ¹⁹Neurogenomics Division, Translational Genomics Research Institute, Phoenix, AZ 85004, USA; ²⁰Institute for Individualized Health (IGNITE), Palo Alto, CA 94301, USA; ²¹Children's Hospital Informatics Program, Children's Hospital Boston and Harvard Medical School, Boston, MA 02115, USA; ²²The Cancer Genome Institute at Fox Chase Cancer Center, Philadelphia, PA 19111, USA; ²³School of Life Sciences, University of Nevada Las Vegas, Las Vegas, NV 89052, USA; ²⁴Bioinformatics Division, The Walter and Eliza Hall Institute of Medical Research, Parkville, Victoria 3052, Australia; ²⁵Oregon Hearing Research Center and Vollum Institute, Oregon Health & Science University, Portland, OR 97239, USA; ²⁶Laboratory of Molecular Genetics, Division of Pediatric Otolaryngology, Head and Neck Surgery, Cincinnati Children's Hospital Research Foundation, and the Department of Otolaryngology, College of Medicine, University of Cincinnati, OH, 45229 USA; ²⁷Interdepartmental PhD Program in Genetics, Department of Otolaryngology, University of Iowa, Iowa City, Iowa City, IA 52242, USA; ²⁸Allama Iqbal Medical College/Jinnah Hospital Complex, University of Health Sciences, Lahore 54550, Pakistan

²⁹These authors contributed equally to this work

*Correspondence: guntram.borck@uk-koeln.de

DOI 10.1016/j.ajhg.2010.12.011. ©2011 by The American Society of Human Genetics. All rights reserved.

cases of early-onset hearing impairment have a genetic cause, with autosomal-recessive inheritance being observed more frequently than autosomal-dominant, X-linked, or mitochondrial inheritance patterns. More than 80 loci for nonsyndromic autosomal-recessive hearing impairment (nonsyndromic ARHI; designated as *DFNB* loci [MIM 220700])⁵ have been mapped and causative mutations have been identified at more than 30 of these loci (Hereditary Hearing Loss Homepage). Genome-wide mapping and identification of genes that are mutated in hearing impairment allows for an unbiased knowledge of proteins and molecular pathways necessary for hearing. This has led to the identification of sets of proteins important for mechanotransduction and the structure of stereocilia, maintenance of high potassium concentrations in the endolymph, and structure and function of the inner ear ribbon synapse and the auditory nerve, among others.² Many genes associated with hearing impairment have been conserved during evolution, and targeted, chemically induced, or knock-down-mediated inactivation of their orthologs in model organisms such as mouse and zebrafish often leads to hearing loss and related phenotypes (e.g., circling behavior).^{6–10} Here, we report the identification of mutations of *ILDR1* (MIM 609739) as the cause of autosomal-recessive hearing impairment *DFNB42* (MIM 609646)¹¹ and evaluate the expression of this gene in mouse and zebrafish.

Subjects and Methods

Family Ascertainment and Clinical Evaluations

The study was approved by the Institutional Review Boards (IRB) at the University of Cologne, Germany; BUITEMS, Quetta, Pakistan; the National Center for Excellence in Molecular Biology (NCEMB), Lahore, Pakistan; the Quaid-I-Azam University, Islamabad, Pakistan; the University of Social Welfare and Rehabilitation Sciences, Tehran, Iran; the Baylor College of Medicine and Affiliated Hospitals, Houston, TX; the University of Iowa, Iowa City, IA; and the Combined Neuroscience IRB at the National Institutes of Health, Bethesda, MD. Written informed consent was obtained from participating individuals or their parents. Some of the hearing-impaired individuals were evaluated by medical history interviews and a physical examination. In general, several affected individuals from each family underwent an otological examination and pure-tone audiometry with air and bone conduction measurements. Some individuals were further evaluated by an ophthalmologic examination with funduscopy and by serum chemistry, blood count, urinalysis, and an electrocardiogram. Blood samples were obtained from each participating individual, and genomic DNA was extracted by standard procedures.

SNP Genotyping and Linkage Analyses

We performed a genome-wide linkage analysis with homozygosity mapping by using Affymetrix GeneChip Human Mapping 250K Sty arrays and genomic DNA samples from consanguineous family PKDF637, which was ascertained in Balochistan province of Western Pakistan. Relationship errors were evaluated with the help of the program Graphical Relationship Representation.¹²

The program PedCheck was applied to detect Mendelian errors¹³ and data for SNPs with such errors were removed from the data set. Non-Mendelian errors were identified with the program MERLIN¹⁴ and unlikely genotypes for related samples were deleted. Linkage analysis was performed assuming autosomal-recessive inheritance, full penetrance, and a disease gene frequency of 0.0001. Multipoint LOD scores were calculated with ALLEGRO,¹⁵ which was also used for haplotype reconstruction. All data handling was performed with the graphical user interface ALOHOMORA.¹⁶ In family PKDF637 and in several other families, we performed fine mapping with short tandem repeat (STR) markers from the chromosome 3q candidate region.

Results of linkage analysis and fine mapping in family DEM4012, the family in which the *DFNB42* locus was originally mapped, have been reported previously.¹¹ A total of 388 STR markers were genotyped in families PKDF223, DEM4089, DEM4098, and DEM4207. Family DEM4430 was genotyped with the Illumina Infinium HumanLinkage-12 Panel, which contains 6090 single-nucleotide polymorphism (SNP) markers. Linkage analysis in families L-867 and L-1621 was performed with 412 STR markers of the Applied Biosystems Linkage mapping set v2.5 and approximately 50,000 SNPs of the Affymetrix 50K XBA GeneChip, respectively. Screening of additional Pakistani families with STR markers from the chromosome 3q13.31-q21.1 region revealed two additional *DFNB42*-linked families, PKDF790 and PKDF899.

Candidate Gene Screening

For candidate gene screening in the linkage interval in family PKDF637, we designed intronic primers to PCR amplify coding exons and the respective exon-intron boundaries by using genomic DNA of an affected individual. Primer pairs for amplification of the eight *ILDR1* coding exons and their approximately 50 base pairs (bp) of flanking intronic sequences (RefSeq accession NM_001199799.1 and GenBank transcript AY672838.1) are listed in Table S1, available online. PCR products were sequenced on an ABI 3730 DNA Analyzer with BigDye chemistry v1.1 or v3.1 (Applied Biosystems). Sequence traces were assembled, aligned, and analyzed with the Seqman software (DNASTAR Lasergene). Mutation nomenclature is based on transcript NM_001199799.1.

Cosegregation of the mutation with deafness in each family was tested by sequencing the respective PCR product amplified from genomic DNA of all participating family members. Depending on the ethnic background of the family for which the candidate mutation was identified, we also sequenced PCR products of 250–500 Pakistani or 60 Iranian individuals.

RT-PCR and In Situ Hybridization Studies in Mouse

RNA was isolated from six organs (cochlea, brain, heart, liver, kidney, and lung) of postnatal day 2 (P2) mice via Trizol (Invitrogen, Darmstadt, Germany).¹⁷ RT-PCR was then performed with primers located in mouse *Ildr1* exons 3 and 7 (primer sequences are listed in Table S1).

Part of the *Ildr1* mRNA (NM_134109) was amplified from murine embryonic day (E) 12.5 otic vesicle with Phusion polymerase (New England Biolabs) via primers located in exons 5 and 7 to yield a 898 bp PCR fragment (primer sequences are listed in Table S1). The PCR product was then cloned into pGEM-T (Promega) and in situ hybridizations were carried out on cochlear sections of P1, P4, and P10 mice as previously described.^{18,19}

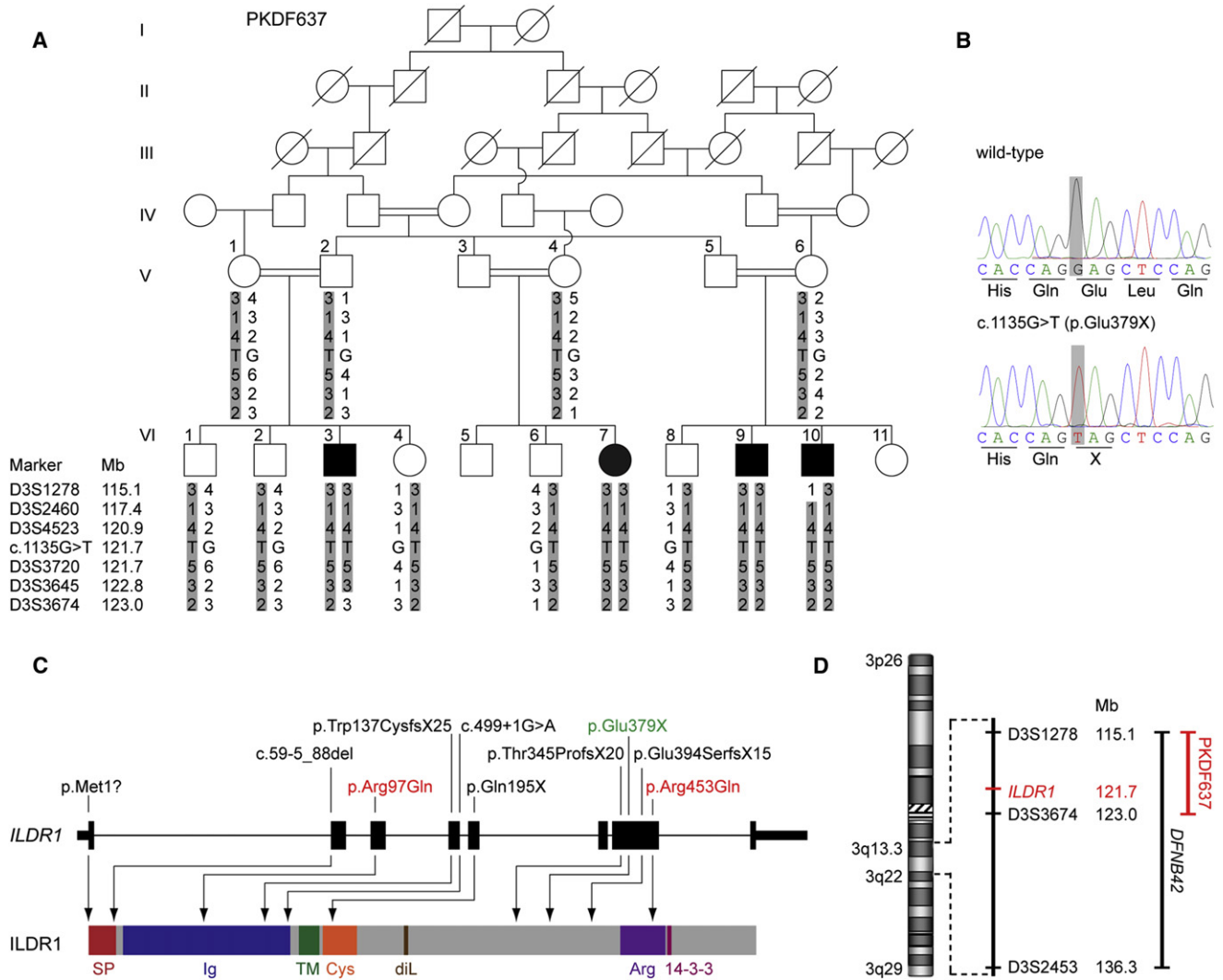


Figure 1. Identification of an *ILDR1* Nonsense Mutation Causing Autosomal-Recessive Hearing Impairment

(A) Pedigree of family PKDF637 and haplotype analysis showing homozygous haplotypes on chromosome 3q13.3-q21.1 in affected individuals. c.1135G>T (NM_001199799.1) denotes an *ILDR1* nonsense mutation leading to p.Glu379X. Mb, megabases from human genome reference sequence build hg19.

(B) Sequence chromatograms of a part of *ILDR1* exon 7 of an individual homozygous for the reference sequence (wild-type) and an affected individual from family PKDF637 homozygous for the c.1135G>T (p.Glu379X) mutation.

(C) Genomic structure of *ILDR1* based on the longest open reading frame (NM_001199799.1) containing eight coding exons (black rectangles). The positions of the ten *ILDR1* mutations are shown both at the gene (top) and the protein level (bottom). The protein diagram depicts the predicted functional domains and sequence motifs. The nonsense mutation identified in family PKDF637 is highlighted in green and the two identified missense substitutions are shown in red. 14-3-3, 14-3-3 binding site; Arg, arginine-rich region; Cys, cysteine-rich region; diL, dileucine motif; Ig, immunoglobulin superfamily domain; SP, signal peptide; TM, transmembrane domain.

(D) Overview of the overlapping linkage intervals on chromosome 3q in family PKDF637 and in the original DFNB42 family (designated DEM4012 in this report).

In Situ Hybridization in Zebrafish

For zebrafish in situ hybridization, the 918 bp *ildr1* EST EE699102.1 (*Danio rerio* cDNA clone IMAGE:8817233) derived from zebrafish whole-body cDNA and cloned into the pExpress-1 vector was purchased from imaGenes (Berlin, Germany). *ildr1* in situ hybridization antisense and control sense probes were generated by in vitro transcription with the SP6 and T7 promoters of the pExpress-1 vector. In situ hybridizations on zebrafish of different stages of development were performed as previously described.²⁰

Results

Identification of a Nonsense Mutation of *ILDR1*

In family PKDF637, four hearing-impaired and seven normal-hearing children were born to three normal-hearing couples who are first or second cousins within a large consanguineous family (Figure 1A), consistent with ARHI. By sequence analysis we found no mutations of *GJB2* (encoding connexin 26; MIM 121011)²¹ and

Table 1. Summary of the Results of Linkage Analysis and *ILDR1* Mutations Detected in 11 Families with Autosomal-Recessive Hearing Impairment

Family ID	Origin	Markers Genotyped	Maximum LOD Score	<i>ILDR1</i> Mutation (cDNA) ^a	Location of the Mutation (Type of Mutation)	<i>ILDR1</i> Mutation (Protein) ^b	Frequency in Control Chromosomes ^c
PKDF637	Pakistan	genome-wide 250k SNP array	5.0	c.1135G>T	exon 7 (nonsense)	p.Glu379X	0/1000
DEM4012 (original DFNB42 family)	Pakistan	genome-wide 388 STR markers	3.7	c.3G>A	exon 1 (start codon)	p.Met1?	0/500
L-1621	Iran	genome-wide 50k SNP array	4.9	c.59-5_88del	intron 1/exon 2 (splice site / deletion)	ND	0/120
PKDF790	Pakistan	<i>DFNB42</i> -linked STRs	5.7	c.290G>A	exon 3 (missense)	p.Arg97Gln	0/692
PKDF223	Pakistan	genome-wide 388 STR markers	2.6	c.411delG ^d	exon 4 (frameshift)	p.Trp137CysfsX25	0/688
				c.1387C>T ^d	exon 7 (missense)	p.Arg463Cys	0/690
DEM4098	Pakistan	genome-wide 388 STR markers	4.6	c.499+1G>A	intron 4 (splice site)	ND	0/688
L-867	Iran	genome-wide 412 STR markers	2.5	c.583C>T	exon 5 (nonsense)	p.Gln195X	0/120
DEM4089	Pakistan	genome-wide 388 STR markers	3.1	c.1032delG	exon 7 (frameshift)	p.Thr345ProfsX20	0/500
DEM4207	Pakistan	genome-wide 388 STR markers	4.0	c.1032delG	exon 7 (frameshift)	p.Thr345ProfsX20	0/500
DEM4430	Pakistan	genome-wide 6k SNP array	4.5	c.1180delG	exon 7 (frameshift)	p.Glu394SerfsX15	0/690
PKDF899	Pakistan	<i>DFNB42</i> -linked STRs	2.1	c.1358G>A	exon 7 (missense)	p.Arg453Gln	0/690

ND, not determined

^a Nucleotide numbering starts from A of the translation initiation ATG codon of transcript NM_001199799.1. All mutations were present in homozygous state in all affected individuals of the respective families.

^b Accession number NP_001186728.1.

^c Ethnically matched controls (Pakistani or Iranian).

^d Two homozygous mutations of *ILDR1* completely cosegregate with deafness in family PKDF223.

SLC26A4 (encoding pendrin; MIM 605646),²² two genes commonly associated with ARHI. We then performed a genome-wide linkage analysis with 250k SNP arrays followed by homozygosity mapping. By using a reduced marker panel of approximately 20,000 SNPs, we identified linkage to a single genomic region on chromosome 3q13.31-q21.1 with a maximum LOD score of 5.0 (Table 1). This LOD score was the maximum expected from simulation analysis, and the region on chromosome 3 was the only region within the genome with a LOD score that exceeded 2.0. With consideration of all SNPs from the 250K SNP array and after haplotype reconstruction, the region of shared homozygosity was determined to be flanked by SNP markers rs16823850 and rs2717225 (data not shown), defining a critical region of 7.6 Mb. The mapping results were confirmed by STR marker genotyping (Figure 1A). The linked region contains 52 annotated known and predicted coding genes and 1 miRNA gene (UCSC Genome Bioinformatics, build hg19). We sequenced *miRNA-198* and 41 coding genes in one affected individual (Table S2), representing approximately 69% of the coding exons, and identified a homozygous nonsynonymous mutation not listed in dbSNP build 131. This mutation is a transversion

(c.1135G>T) located in exon 7 of *ILDR1* and is predicted to lead to a premature stop codon (p.Glu379X; Figure 1B; Table 1). This nonsense mutation cosegregated with ARHI in the family as expected from the haplotype analysis (Figure 1A) and was not likely to be a polymorphism because it is absent not only from dbSNP but also from the 1000 Genomes database. We also did not find it in 1000 Pakistani control chromosomes (Table 1).

ILDR1, a gene of unknown function, encodes the immunoglobulin-like domain containing receptor 1, a predicted type 1 transmembrane protein.²³ Alternative splicing produces up to five different transcripts, four of which have been reported previously,^{23,24} an additional mRNA being annotated in the UCSC Genome Browser (AY134857.1; Figure S1). The longest *ILDR1* open reading frame consists of eight coding exons and encodes a 546 amino acid protein. *ILDR1* is predicted to contain a signal peptide, an extracellular immunoglobulin (Ig) superfamily domain, and a transmembrane domain as well as other predicted functional domains such as a cysteine-rich and an arginine-rich domain, an LSR (lipolysis stimulated lipoprotein receptor) domain, a dileucine motif, and a 14-3-3 binding site (Figure 1C).²³ Isoforms lacking the dileucine

motif or the transmembrane domain have been identified but the tissue distribution, and functional significance of the putative membrane-bound and soluble *ILDR1* isoforms are unknown. The p.Glu379X alteration located in exon 7 affects four *ILDR1* isoforms (Figure S1) and might render the transcripts susceptible to nonsense-mediated mRNA decay (NMD). No RNA from an affected individual of family PKDF637 was available to test this hypothesis. If the protein is expressed, it would lack the arginine-rich region and the predicted 14-3-3 binding site (Figure 1C).

***ILDR1* Mutation in the Original DFNB42 Family**

ILDR1 is contained within the 21.1 Mb *DFNB42* interval defined by linkage analysis in an unrelated Pakistani family segregating ARHI (family DEM4012; Figure 1D; Table 1).¹¹ To determine whether an *ILDR1* mutation causes deafness also in the original DFNB42 family DEM4012, we sequenced the *ILDR1* coding exons and splice sites in an affected family member. We identified a homozygous start codon mutation (c.3G>A [p.Met1?]; Table 1; Figure S2). This variant cosegregated with autosomal-recessive/pseudodominant hearing impairment (Figure 2A) and was not found in 500 Pakistani control chromosomes. Therefore, we conclude that *ILDR1* is the gene mutated in DFNB42 hearing impairment.

Although the consequences of this mutation at the transcript and protein level are unknown, we note that Met136 is the next downstream in-frame methionine that might be used as a translation initiation codon, possibly leading to an N-terminal protein truncation. However, Met136 does not show a strong Kozak consensus sequence (G at position -3 but a T instead of a consensus G at position +4). Alternatively, MutationTaster²⁵ predicts use of the next downstream ATG, which indeed shows a strong Kozak consensus sequence but is out-of-frame, potentially producing a 43 amino acid polypeptide with no similarity to *ILDR1*.

***ILDR1* Mutations in Autosomal-Recessive Hearing Impairment**

We next sequenced *ILDR1* in affected individuals of nine additional unrelated ARHI families. These families were identified either by targeted screening for linkage to STR markers at the *DFNB42* locus or through genome-wide homozygosity mapping with LOD scores ranging from 2.1 to 5.7 at this locus (Table 1). Seven of nine DFNB42 families originated from different regions in Pakistan and two are from Iran. We identified a homozygous *ILDR1* mutation in affected individuals from all nine families. In total we identified eight different homozygous *ILDR1* mutations, one mutation being present in two families. The mutant alleles included one nonsense and one canonical splice donor site mutation, two missense variants, three frameshift mutations leading to premature stop codons, and a 35 bp deletion that removes 5 bp at the exon 2 splice acceptor site and extends for 30 bp into exon 2 (Figures 2B–2J; Table 1; sequence chromatograms

are shown in Figure S2). All mutations cosegregated with hearing impairment in the respective families and none of them were present in dbSNP, in the 1000 Genomes database, or in 120 to 692 chromosomes from ethnically matched controls (Figures 2B–2J; Table 1).

One frameshift mutation (c.1032delG [p.Thr345ProfsX20]) was present in two apparently unrelated Pakistani families (DEM4089 and DEM4207) and STR genotyping indicated that affected individuals from both families shared identical haplotypes at three STR markers including the *ILDR1* intragenic marker D3S3720 (data not shown), suggesting that the mutation was inherited from a common ancestor of the two families. Two missense substitutions replaced arginine residues at positions 97 and 453 with glutamine. Whereas the p.Arg97Gln change (c.290G>A) is located in the Ig superfamily domain (Figure 1C) and is predicted to be “possibly damaging” by PolyPhen and “not tolerated” by SIFT, p.Arg453Gln (c.1358G>A) was identified in the family with the lowest LOD score of all 11 families (2.1; Table 1) and is predicted to be benign by PolyPhen and SIFT. Multiple species sequence alignments confirmed a high degree of conservation of Arg97 among *ILDR1* orthologs and paralogs whereas Arg453 is moderately conserved (Figure S3). Thus, confirmation of the possible pathogenicity of p.Arg453Gln awaits future functional analyses. However, we note that p.Arg453Gln was not observed in 690 control chromosomes (Table 1), arguing for its pathogenicity. Furthermore, Arg453 is one of the arginine residues of the arginine-rich region located at amino acid positions 431–466 of the 546 residue isoform (Figure 1C). Although the function(s) of arginine-rich regions are not comprehensively documented, some can mediate protein-protein interactions²⁶ and substitution of critical arginine residues might impede this function.

A third homozygous missense substitution, p.Arg463Cys (encoded by c.1387C>T), cosegregated with deafness in family PKDF223. However, affected family members are also homozygous for a truncating *ILDR1* mutation, which we consider sufficient to cause deafness, so a possible pathogenic effect of p.Arg463Cys alone is speculative. In conclusion, multiple mutant alleles of *ILDR1* are distributed across the gene (Figure 1C), and a majority of them are truncating mutations that might induce NMD and/or produce likely nonfunctional truncated proteins.

Clinical Characterization of DFNB42 Hearing Impairment

All individuals homozygous for an *ILDR1* mutation had sensorineural hearing impairment. Hearing impairment was prelingual (and possibly congenital), bilateral, and of moderate-to-profound severity. Representative audiograms are shown in Figure 3 and complete audiogram data of three families are presented in Figure S4. In most affected individuals, hearing impairment was more pronounced at higher frequencies (“sloping” audiogram; Figure 3A), but in some patients all frequencies were similarly affected, giving rise to a “flat” audiogram (Figure 3B). Although no

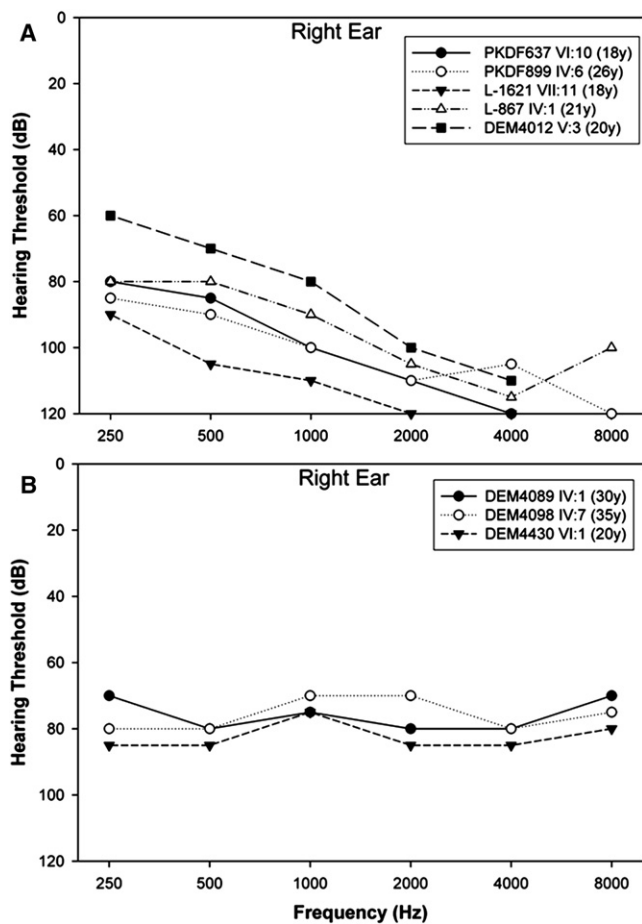


Figure 3. Representative Audiograms of Hearing-Impaired Individuals Homozygous for *ILDR1* Mutations

(A) Audiograms of selected individuals from families PKDF637, PKDF899, L-1621, L-867, and DEM4012 showing hearing impairment that is more pronounced at high frequencies.

(B) Audiograms of selected individuals from families DEM4089, DEM4098, and DEM4430 showing hearing impairment involving all frequencies similarly. Only audiograms measured from the right ear are shown. Audiograms from the left ear were similar. y, age at time of audiogram in years.

neuropathy. No subjective vestibular symptoms were reported. Thus, we conclude that *ILDR1* mutations cause bilateral nonprogressive moderate-to-profound sensorineural hearing impairment.

Hearing impairment appeared nonsyndromic because no associated congenital anomalies, facial dysmorphisms, or intellectual disabilities were reported by the families or detected on physical examination. Several affected individuals underwent detailed clinical and laboratory examinations, and all were normal. The most comprehensive investigations were performed in the male individual IV:6 from family PKDF899 at the age of 26 years. No anomalies were detected in blood chemistry (including urea nitrogen and creatinine), thyroid function test, and urinalysis, and there was no ophthalmological involvement (normal funduscopy) and no cardiac arrhythmia as assessed by an electrocardiogram.

Expression of *Ildr1* in the Mouse Inner Ear

ILDR1 is expressed in human prostate, testis, pancreas, kidney, heart, and liver,²³ and the UniGene database (entry Mm.17807) contains an *Ildr1* EST (BQ568480.1) derived from the mouse inner ear. Consistent with these observations, massively parallel signature sequencing (MPSS) of mouse transcripts has previously revealed *Ildr1* expression in the inner ear and in a few other tissues.²⁷ However, expression of *Ildr1* in the various cell types of the cochlea has not been investigated. The centromeric part of the *DFNB42* linkage region on chromosome 3q13.31-q22.3 shows conserved synteny with mouse chromosome 16qB3 where the orthologous *Ildr1* gene is located. Because human *ILDR1* and mouse *Ildr1* mRNAs are highly similar with 81% sequence identity at the nucleotide level (79% sequence identity at the protein level), we investigated *Ildr1* expression in the mouse cochlea as a model system. Expression of *Ildr1* was first examined in P2 mouse organs by nonquantitative RT-PCR. We detected *Ildr1* expression in all tissues tested, including the cochlea (Figure 4A). In this experimental setting, the most abundant transcript contained exon 6, potentially representing a transcript encoding the mouse full-length 537 amino acid isoform.

To determine the spatio-temporal expression pattern of *Ildr1* in the mouse inner ear, we performed mRNA in situ hybridization experiments on P1, P4, and P10 mice. *Ildr1* mRNA was detected in the cochlea and the vestibule at P4 (Figures 4B–4E and Figure S5, respectively). Expression in the organ of Corti was low at P1 (Figures 4F–4H) and increased gradually at P4 and P10 (Figures 4I–4N). Expression was detected at low-to-intermediate levels in hair cells and at higher levels in a subset of supporting cells (Figures 4F, 4I, and 4L). Supporting cells expressing high levels of *Ildr1* at P4 are presumably the Pillar cells and a subset of Hensen cells (Figures 4I and 4O). A schematic overview of the *Ildr1* expression pattern in the mouse organ of Corti at P4 is given in Figure 4O.

Expression of *ildr1* in Zebrafish

In the zebrafish genome (build Zv9), a single *ILDR1* ortholog is annotated. *Danio rerio* *ildr1* shares 40% amino acid sequence identity with human *ILDR1*. A BLAST search²⁸ of the nonredundant (NR) protein database with the human full-length 546 amino acid *ILDR1* sequence identified *ildr1* and a second protein, the product of *zgc:64227*, as putative *ILDR1* orthologs in zebrafish. *ildr1* and its paralog encoded by *zgc:64227* share 47% sequence identity at the amino acid level and are presumably derived from a single ancestral gene after the genome duplication that has occurred in the fish lineage (Figure S6). Although *zgc:64227* has previously been shown to be expressed in the zebrafish otic placode at the 14–19 somite stage (corresponding to 16–19 hr postfertilization [hpf]) and in the lateral line from the 20–25 somite stage (19–22 hpf) on (ZFIN homepage), the tissue distribution of *ildr1* has not been determined. Therefore, we performed *ildr1* whole-mount in situ hybridization in wild-type zebrafish

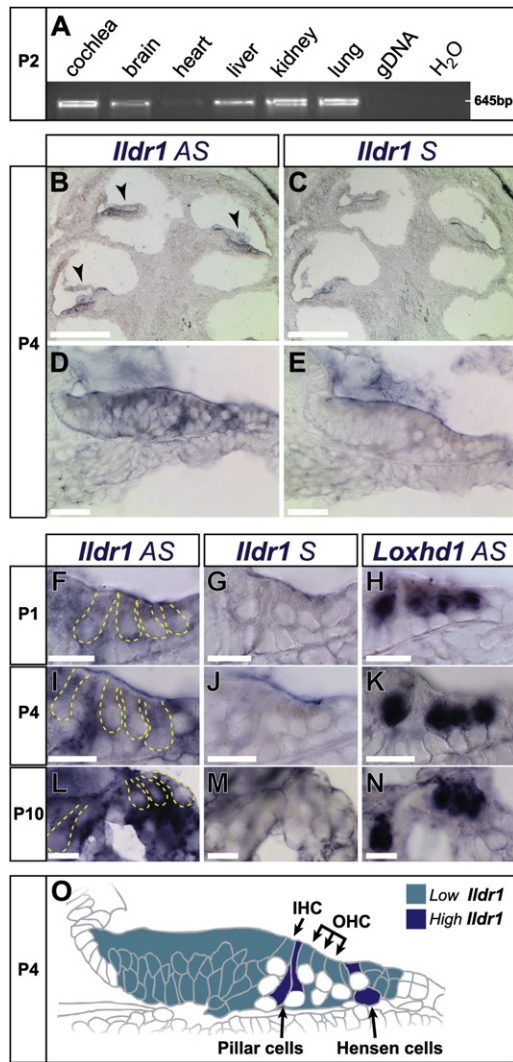


Figure 4. Expression of *Ildr1* in the Mouse Inner Ear

(A) Nonquantitative RT-PCR with exonic *Ildr1* primers on cDNA derived from P2 mouse organs. gDNA, genomic DNA; H₂O, control PCR with water as a template.

(B–E) In situ hybridization of *Ildr1* in the mouse cochlea at P4. Antisense (AS) probe (B and D); control sense (S) probe (C and E). Arrowheads in (B) point at the organ of Corti.

(F–N) In situ hybridization of *Ildr1* in the organ of Corti at high magnification at P1 (F–H), P4 (I–K), and P10 (L–N) with *Ildr1* antisense (F, I, L) and sense (G, J, M) probes. Yellow dotted lines in (F), (I), and (L) indicate the positions of inner and outer hair cells. *Ildr1* is expressed at low-to-intermediate levels in hair cells and at higher levels in the Pillar and Hensen cells adjacent to hair cells. In (H), (K), and (N), the hair cells are stained with a *Loxhd1* antisense probe, which is used as a positive control (i.e., *Loxhd1* is highly expressed in hair cells).¹⁸

(O) Diagram of *Ildr1* expression in the mouse organ of Corti at P4. IHC, inner hair cell; OHC, outer hair cells.

Scale bars represent 200 μm in (B) and (C), 100 μm in (D) and (E), and 20 μm in (F)–(N).

embryos and larvae between early segmentation stages (11 hpf) and day 6 of development. No distinct signal was obtained with the control sense probe (data not shown). We did not detect *ildr1* expression at 11 hpf. At 15 hpf, however, a weak signal was present in the developing

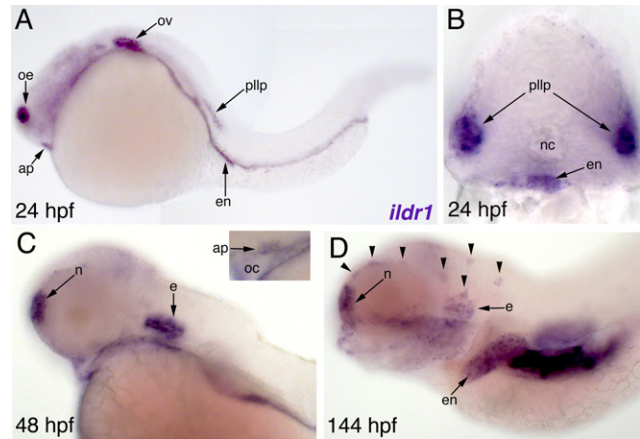


Figure 5. Expression of *ildr1* in Zebrafish

Whole-mount in situ hybridization with probes for *ildr1* transcripts in wild-type zebrafish embryos and larvae at ages indicated in the bottom left corners. (A, C, D) Lateral views with anterior to the left. (B) Cross section at the level of the posterior lateral line primordium. The inset in (C) depicts a magnification of the *ildr1*-positive anterior pituitary gland of the 48 hpf larvae. Arrowheads in (D) point to neuromasts, the sensory organs of the lateral line system. ap, anterior pituitary; e, ear; en, endoderm; n, nose; nc, notochord; oc, oral cavity; oe, olfactory epithelium; ov, otic vesicle; pllp, posterior lateral line primordium.

endoderm (data not shown), and a broader expression pattern can be seen from 24 hpf onward (Figure 5). At this stage, *ildr1* is expressed in several derivatives of the preplacodal ectoderm including the adenohypophyseal placode, the olfactory epithelium and, notably, the otic vesicle and the primordium of the posterior lateral line, which later gives rise to the neuromast-containing lateral line organ (Figures 5A and 5B). In addition, transcripts can be detected in the developing gastrointestinal duct (Figures 5A and 5B). *ildr1* expression persists at least up to day 6 (144 hpf) in the endoderm, the nose, the neuromasts (which are the sensory organs of the lateral line), and in the ear where expression is high at 48 hpf (Figures 5C and 5D). Notably, the otic vesicle from approximately 20 hpf onward, the ear, and the lateral line primordium contain hair cells.⁸

Discussion

We have identified mutations of *ILDR1* underlying autosomal-recessive nonsyndromic hearing impairment at the *DFNB42* locus. Seven of ten distinct *ILDR1* mutations are nonsense, frameshift, or splice site mutations predicted to introduce premature stop codons that may lead to NMD and/or protein truncation. Thus, complete loss of *ILDR1* function appears to underlie hearing impairment in most if not all cases. The *DFNB42* locus was originally mapped in a single Pakistani family.¹¹ Our identification of *ILDR1* mutations in nine Pakistani and two Iranian families raises the possibility that mutations of *ILDR1* may be among the more prevalent causes of ARHI, a genetically highly heterogeneous condition. On the other hand, the large allelic heterogeneity at the *DFNB42* locus in families from

Pakistan alone is similar to allelic heterogeneity for other genes associated with hearing impairment that have been extensively studied in this population.^{21,22}

ILDR1 belongs to an evolutionarily conserved family of Ig domain-containing proteins of unknown function. Mouse *Ildr2* (also known as *Lisch-like*) has been reported as a type 2 diabetes susceptibility gene in DBA mice.²⁹ Another homolog, *LSR*, encodes the lipolysis-stimulated lipoprotein receptor that binds free fatty acids and contributes to the control of plasma triglyceride and cholesterol levels.^{30,31} Notably, the zebrafish *ildr2* ortholog is highly expressed in the otic vesicle at 24 hpf and the ear at 48 hpf.²⁹ We note that human *ILDR2* maps to the *DFNA7* locus on 1q24.1³² and is therefore an interesting candidate gene for autosomal-dominant deafness. Although the function of *ILDR1* remains elusive,²³ its expression in the mouse cochlea and vestibule as well as in the zebrafish ear and in lateral line neuromasts supports an essential role in hearing in vertebrates. A necessary function of *ILDR1* only for hearing is supported by the lack of obvious additional clinical signs outside the auditory system in affected individuals despite the wide tissue distribution of *ILDR1*. This is not an unusual observation; there are mutant alleles of several ubiquitously expressed genes associated with nonsyndromic deafness such as *TPRN* (MIM 613354), *MARVELD2* (also known as *TRIC*, MIM 610572), *HGF* (MIM 142409), and *ACTG1* (MIM 102560).^{17,33–36}

Many genes that are mutated in DFNB hearing impairment are highly expressed in cochlear hair cells and predominant expression in supporting cells is an exception.³⁷ Our *in situ* hybridization experiments in the mouse inner ear show that *Ildr1* is weakly expressed in hair cells and at higher levels in a subset of supporting cells. Whether *DFNB42*-linked hearing impairment is due to disruption of *ILDR1* function in hair cells, supporting cells, or both remains to be addressed in future studies.

In conclusion, mutations of *ILDR1* constitute a previously unreported cause of DFNB hearing impairment. *ILDR1* is a gene of unknown function but with a consistent expression pattern in auditory and vestibular tissues in mouse and zebrafish. Future studies will address the spectrum and prevalence of *ILDR1* mutations in ARHI families of different ethnic and geographical origins, the localization of the *ILDR1* protein in the mammalian cochlea, the tissue distribution and functions of the different *ILDR1* isoforms and possible ligands, interaction partners, and downstream effectors of this putative transmembrane receptor.

Supplemental Data

Supplemental Data include six figures and two tables and can be found with this article online at <http://www.cell.com/AJHG/>.

Acknowledgments

We wish to thank the family members for their invaluable participation and cooperation. We thank Dennis Drayna and Changsoo

Kang for critically reading the manuscript. This work was funded by the Deutsche Forschungsgemeinschaft (DFG; BO2985/3-1; to G.B.), the European Commission FP6 Integrated Project EURO-HEAR, Grant LSHG-CT-20054-512063 (to B.W. and C.K.), NIH RO1 DC002842 (to R.J.H.S.), NHMRC Career Development Award (to M.B.), NHMRC Overseas Biomedical Fellowship (to M.S.H.), Doris Duke Fellowship (to A.E.S.), NIH DC007704 and Skaggs Institute for Chemical Biology (to U.M.), NIH intramural funds from NIDCD DC000039-14 (to T.B.F.), Higher Education Commission (HEC), Government of Pakistan (to W.A.), NIH-NIDCD grant DC03594 (to S.M.L.), and the ICGEB, Trieste, Italy (to Sheikh R.). J.A. thanks Dost Muhammad Baloch and Ahmed Farooq Bazai, VC, BUIITEMS, for faculty funds. Genotyping services were partially provided by the Center for Inherited Disease Research (CIDR). CIDR is fully funded through a federal contract from the NIH to The Johns Hopkins University, Contract Number N01-HG-65403 (to S.M.L.).

Received: November 17, 2010

Revised: December 16, 2010

Accepted: December 20, 2010

Published online: January 20, 2011

Web Resources

The URLs for data presented herein are as follows:

1000 Genomes browser, <http://browser.1000genomes.org/index.html>

dbSNP, <http://www.ncbi.nlm.nih.gov/projects/SNP>

GenBank, <http://www.ncbi.nlm.nih.gov/genbank>

Hereditary Hearing Loss home page, <http://hereditaryhearingloss.org>

MutationTaster, <http://www.mutationtaster.org/>

Online Mendelian Inheritance in Man (OMIM), <http://www.ncbi.nlm.nih.gov/Omim/>

Polyphen, <http://genetics.bwh.harvard.edu/pph>

Sorting Intolerant from Tolerant (SIFT), <http://sift.jcvi.org>

TMHMM (prediction of transmembrane helices in proteins), <http://www.cbs.dtu.dk/services/TMHMM>

UCSC Genome Bioinformatics, <http://www.genome.ucsc.edu>

UniGene, <http://www.ncbi.nlm.nih.gov/unigene>

ZFIN, http://zfin.org/cgi-bin/webdriver?Mival=aa-ZDB_home.app

References

1. Fritsch, B., Beisel, K.W., and Bermingham, N.A. (2000). Developmental evolutionary biology of the vertebrate ear: Conserving mechanoelectric transduction and developmental pathways in diverging morphologies. *Neuroreport* 11, R35–R44.
2. Dror, A.A., and Avraham, K.B. (2010). Hearing impairment: A panoply of genes and functions. *Neuron* 68, 293–308.
3. Gillespie, P.G., and Muller, U. (2009). Mechanotransduction by hair cells: Models, molecules, and mechanisms. *Cell* 139, 33–44.
4. Frolenkov, G.I., Belyantseva, I.A., Friedman, T.B., and Griffith, A.J. (2004). Genetic insights into the morphogenesis of inner ear hair cells. *Nat. Rev. Genet.* 5, 489–498.
5. Petersen, M.B., and Willems, P.J. (2006). Non-syndromic, autosomal-recessive deafness. *Clin. Genet.* 69, 371–392.
6. Brown, S.D., Hardisty-Hughes, R.E., and Mburu, P. (2008). Quiet as a mouse: Dissecting the molecular and genetic basis of hearing. *Nat. Rev. Genet.* 9, 277–290.

7. Leibovici, M., Safieddine, S., and Petit, C. (2008). Mouse models for human hereditary deafness. *Curr. Top. Dev. Biol.* 84, 385–429.
8. Nicolson, T. (2005). The genetics of hearing and balance in zebrafish. *Annu. Rev. Genet.* 39, 9–22.
9. Nicolson, T., Rusch, A., Friedrich, R.W., Granato, M., Ruppertsberg, J.P., and Nusslein-Volhard, C. (1998). Genetic analysis of vertebrate sensory hair cell mechanosensation: The zebrafish circler mutants. *Neuron* 20, 271–283.
10. Vrijens, K., Van Laer, L., and Van Camp, G. (2008). Human hereditary hearing impairment: Mouse models can help to solve the puzzle. *Hum. Genet.* 124, 325–348.
11. Aslam, M., Wajid, M., Chahrour, M.H., Ansar, M., Haque, S., Pham, T.L., Santos, R.P., Yan, K., Ahmad, W., and Leal, S.M. (2005). A novel autosomal recessive nonsyndromic hearing impairment locus (DFNB42) maps to chromosome 3q13.31-q22.3. *Am. J. Med. Genet. A.* 133A, 18–22.
12. Abecasis, G.R., Cherny, S.S., Cookson, W.O., and Cardon, L.R. (2001). GRR: Graphical representation of relationship errors. *Bioinformatics* 17, 742–743.
13. O'Connell, J.R., and Weeks, D.E. (1998). PedCheck: A program for identification of genotype incompatibilities in linkage analysis. *Am. J. Hum. Genet.* 63, 259–266.
14. Abecasis, G.R., Cherny, S.S., Cookson, W.O., and Cardon, L.R. (2002). Merlin—Rapid analysis of dense genetic maps using sparse gene flow trees. *Nat. Genet.* 30, 97–101.
15. Gudbjartsson, D.E., Jonasson, K., Frigge, M.L., and Kong, A. (2000). Allegro, a new computer program for multipoint linkage analysis. *Nat. Genet.* 25, 12–13.
16. Ruschendorf, F., and Nurnberg, P. (2005). ALOHOMORA: A tool for linkage analysis using 10K SNP array data. *Bioinformatics* 21, 2123–2125.
17. Li, Y., Pohl, E., Boulouiz, R., Schradlers, M., Nurnberg, G., Charif, M., Admiraal, R.J., von Ameln, S., Baessmann, I., Kandil, M., et al. (2010). Mutations in TPRN cause a progressive form of autosomal-recessive nonsyndromic hearing loss. *Am. J. Hum. Genet.* 86, 479–484.
18. Grillet, N., Schwander, M., Hildebrand, M.S., Sczaniecka, A., Kolatkar, A., Velasco, J., Webster, J.A., Kahrizi, K., Najmabadi, H., Kimberling, W.J., et al. (2009). Mutations in LOXHD1, an evolutionarily conserved stereociliary protein, disrupt hair cell function in mice and cause progressive hearing loss in humans. *Am. J. Hum. Genet.* 85, 328–337.
19. Schwander, M., Sczaniecka, A., Grillet, N., Bailey, J.S., Avenarius, M., Najmabadi, H., Steffy, B.M., Federe, G.C., Lagler, E.A., Banan, R., et al. (2007). A forward genetics screen in mice identifies recessive deafness traits and reveals that pejvakin is essential for outer hair cell function. *J. Neurosci.* 27, 2163–2175.
20. Hammerschmidt, M., Pelegri, F., Mullins, M.C., Kane, D.A., van Eeden, F.J., Granato, M., Brand, M., Furutani-Seiki, M., Haffter, P., Heisenberg, C.P., et al. (1996). dino and mercedes, two genes regulating dorsal development in the zebrafish embryo. *Development* 123, 95–102.
21. Santos, R.L., Wajid, M., Pham, T.L., Hussan, J., Ali, G., Ahmad, W., and Leal, S.M. (2005). Low prevalence of Connexin 26 (GJB2) variants in Pakistani families with autosomal recessive non-syndromic hearing impairment. *Clin. Genet.* 67, 61–68.
22. Anwar, S., Riazuddin, S., Ahmed, Z.M., Tasneem, S., Jaleel, A.u., Khan, S.Y., Griffith, A.J., Friedman, T.B., and Riazuddin, S. (2009). SLC26A4 mutation spectrum associated with DFNB4 deafness and Pendred's syndrome in Pakistanis. *J. Hum. Genet.* 54, 266–270.
23. Hauge, H., Patzke, S., Delabie, J., and Aasheim, H.C. (2004). Characterization of a novel immunoglobulin-like domain containing receptor. *Biochem. Biophys. Res. Commun.* 323, 970–978.
24. Strausberg, R.L., Feingold, E.A., Grouse, L.H., Derge, J.G., Klausner, R.D., Collins, F.S., Wagner, L., Shenmen, C.M., Schuler, G.D., Altschul, S.F., et al. (2002). Generation and initial analysis of more than 15,000 full-length human and mouse cDNA sequences. *Proc. Natl. Acad. Sci. USA* 99, 16899–16903.
25. Schwarz, J.M., Rödelsperger, C., Schuelke, M., and Seelow, D. (2010). MutationTaster evaluates disease-causing potential of sequence alterations. *Nat. Methods* 7, 575–576.
26. Brodeur, J., Larkin, H., Boucher, R., Thériault, C., St-Louis, S.C., Gagnon, H., and Lavoie, C. (2009). Calnuc binds to LRP9 and affects its endosomal sorting. *Traffic* 10, 1098–1114.
27. Peters, L.M., Belyantseva, I.A., Lagziel, A., Battey, J.F., Friedman, T.B., and Morell, R.J. (2007). Signatures from tissue-specific MPSS libraries identify transcripts preferentially expressed in the mouse inner ear. *Genomics* 89, 197–206.
28. McGinnis, S., and Madden, T.L. (2004). BLAST: At the core of a powerful and diverse set of sequence analysis tools. *Nucleic Acids Res.* 32, W20–W25.
29. Dokmanovic-Chouinard, M., Chung, W.K., Chevre, J.C., Watson, E., Yonan, J., Wiegand, B., Bromberg, Y., Wakae, N., Wright, C.V., Overton, J., et al. (2008). Positional cloning of “Lisch-Like”, a candidate modifier of susceptibility to type 2 diabetes in mice. *PLoS Genet.* 4, e1000137.
30. Narvekar, P., Berriel Diaz, M., Krones-Herzig, A., Hardeland, U., Strzoda, D., Stohr, S., Frohme, M., and Herzig, S. (2009). Liver-specific loss of lipolysis-stimulated lipoprotein receptor triggers systemic hyperlipidemia in mice. *Diabetes* 58, 1040–1049.
31. Yen, F.T., Roitel, O., Bonnard, L., Notet, V., Pratte, D., Stenger, C., Magueur, E., and Bihain, B.E. (2008). Lipolysis stimulated lipoprotein receptor: A novel molecular link between hyperlipidemia, weight gain, and atherosclerosis in mice. *J. Biol. Chem.* 283, 25650–25659.
32. Fagerheim, T., Nilssen, O., Raeymaekers, P., Brox, V., Moum, T., Elverland, H.H., Teig, E., Omland, H.H., Fostad, G.K., and Tranebjaerg, L. (1996). Identification of a new locus for autosomal dominant non-syndromic hearing impairment (DFNA7) in a large Norwegian family. *Hum. Mol. Genet.* 5, 1187–1191.
33. Rehman, A.U., Morell, R.J., Belyantseva, I.A., Khan, S.Y., Boger, E.T., Shahzad, M., Ahmed, Z.M., Riazuddin, S., Khan, S.N., Riazuddin, S., and Friedman, T.B. (2010). Targeted capture and next-generation sequencing identifies C9orf75, encoding taperin, as the mutated gene in nonsyndromic deafness DFNB79. *Am. J. Hum. Genet.* 86, 378–388.
34. Riazuddin, S., Ahmed, Z.M., Fanning, A.S., Lagziel, A., Kitajiri, S., Ramzan, K., Khan, S.N., Chattaraj, P., Friedman, P.L., Anderson, J.M., et al. (2006). Tricellulin is a tight-junction protein necessary for hearing. *Am. J. Hum. Genet.* 79, 1040–1051.
35. Schultz, J.M., Khan, S.N., Ahmed, Z.M., Riazuddin, S., Warayah, A.M., Chhatre, D., Starost, M.F., Ploplis, B., Buckley, S., Velasquez, D., et al. (2009). Noncoding mutations of HGF are associated with nonsyndromic hearing loss, DFNB39. *Am. J. Hum. Genet.* 85, 25–39.

36. Zhu, M., Yang, T., Wei, S., DeWan, A.T., Morell, R.J., Efenbein, J.L., Fisher, R.A., Leal, S.M., Smith, R.J., and Friderici, K.H. (2003). Mutations in the gamma-actin gene (ACTG1) are associated with dominant progressive deafness (DFNA20/26). *Am. J. Hum. Genet.* *73*, 1082–1091.
37. Wilcox, E.R., Burton, Q.L., Naz, S., Riazuddin, S., Smith, T.N., Ploplis, B., Belyantseva, I., Ben-Yosef, T., Liburd, N.A., Morell, R.J., et al. (2001). Mutations in the gene encoding tight junction claudin-14 cause autosomal recessive deafness DFNB29. *Cell* *104*, 165–172.